Available online at www.sciencedirect.com
SCIENCE DIRECT®
International Journal of Thermal Sciences 45 (2006) 494–503
International Journal of Thermal Sciences
www.elsevier.com/locate/ijts

Modeling of trichlorofluoromethane hydrate formation in a w/o emulsion submitted to steady cooling

Juan Ramón Avendaño-Gómez [a,*], Roberto Limas-Ballesteros [a], Fernando García-Sánchez [b]

[a] *Laboratorio de Investigación en Ingeniería Química Ambiental, SEPI-ESIQIE, Instituto Politécnico Nacional, Unidad Profesional Adolfo López Mateos, Zacatenco, Edificio 8, 3er piso 07738, México DF, Mexico*
[b] *Laboratorio de Termodinámica, Programa de Ingeniería Molécular, Instituto Mexicano del Petróleo, Eje Central Lázaro Cárdenas 152, 07730 México DF, Mexico*

Received 6 December 2004; received in revised form 22 June 2005; accepted 22 June 2005

Available online 5 August 2005

Abstract

The aim of this work is to study the modeling of the thermal evolution inside an hydrate forming system which is submitted to an imposed steady cooling. The study system is a w/o emulsion where the formulation considers the CCl_3F as the hydrate forming molecule dissolved in the oil phase. The hydrate formation occurs in the aqueous phase of the emulsion, i.e. in the dispersed phase. The model equation is based on the resolution of the continuity equation in terms of a heat balance for the dispersed phase. The crystallization of the CCl_3F hydrate occurs at supercooling conditions ($T_c < T_F$), besides, the heat released during crystallization interferes with the imposed condition of steady decrease of temperature around the system. Thus, the inclusion of the heat source term has to be considered in order to take into account the influence of crystallization. The rate of heat released during the crystallization is governed by the probability of nucleation $J(T)$. Previous experimental measurements allowed to derive the corresponding function $J(T)$ of the w/o emulsion. The results provided by the model equation subjected to boundary conditions allow to depict the evolution of temperature in the dispersed phase. The most singular point in the temperature–time curve is the onset time of hydrate crystallization. Three time intervals characterize the evolution of temperature during the steady cooling of the w/o emulsion: (1) steady cooling, (2) hydrate formation with a release of heat, (3) a last interval of steady cooling.

Keywords: Hydrate formation; Supercooling; Crystallization; W/o emulsion; Trichlorofluoromethane hydrate

1. Introduction

Gas hydrates or clathrate hydrates are one class of inclusion compounds. The formation of a clathrate hydrate is the result of a kinetic process of crystallization that releases heat during the phase change. Besides, the hydrate formation normally occurs at lower temperatures than the equilibrium temperatures. Such a difference between the theoretical equilibrium conditions of hydrate crystallization and actual temperature T and chemical potential $\Delta\mu$ of hydrate crystallization is due to the stochastic nature of nucleation.

In a previous work [1] we presented the experimental results of hydrate formation in a w/o emulsion studied by differential scanning calorimetry (DSC). Now, in this work the objective is to determine the thermal evolution of the aqueous dispersed phase which is the locus of hydrate formation. The mathematical model equation is based on the resolution of the continuity equation in terms of a heat balance. The boundary volume of the model is a cylindrical geometry of a few mm^3, such geometry corresponds to the crucible employed in DSC. In the continuity equation the heat source term is taken into consideration because an amount of heat is released during the hydrate crystallization. The convective term of bulk flow is not considered within the model, only heat transfer by conduction is taken into consideration.

* Corresponding author.
E-mail address: juan_avendan@yahoo.com.mx (J.R. Avendaño-Gómez).

1290-0729/$ – see front matter
doi:10.1016/j.ijthermalsci.2005.06.007

Nomenclature

A	coefficient in function $J(T)$
B	coefficient in function $J(T)$
Cp_s	specific heat of the dispersed phase in solid phase
Cp_l	specific heat of the dispersed phase in liquid phase
ΔG	Gibbs free energy
E	coefficient in function $J(T)$
i	radial position in discretized terms
J	rate of nucleation
k	Boltzman constant
k in text	global heat transfer coefficient
L	apparent latent heat of the dispersed phase
m	time in discretized terms
M	final time of the cooling experiment in discretized terms
N	total number of dispersed droplets
n	number of crystallized droplets
$\dot{q}$	rate of heat released by the dispersed phase
r	radial coordinate
R	radius of the cylinder
t	time
t_{end}	final time of the cooling experiment
T_F	melting temperature of the dispersed phase
T_{end}	lower limit of temperature of the cooling experiment
T_c^*	most likely crystallization temperature of the dispersed phase

Greek symbols

β	cooling rate
λ_l	thermal conductivity of the dispersed phase in liquid state
λ_s	thermal conductivity of the dispersed phase in solid state
φ	fraction of solidified droplets
Φ	mass fraction of dispersed phase in the w/o emulsion
Θ	temperature in discretized terms
μ	chemical potential
ρ	density of the dispersed phase

The study system is a water-in-oil emulsion (w/o emulsion), the hydrate forming molecule is trichlorofluoromethane CCl_3F in liquid state dissolved as a solute in the oil phase of the w/o emulsion. The dispersed phase is a population of aqueous micro-droplets (mean droplet diameter 60 μm). A necessary process to initiate the kinetic process of hydrate formation is the molecular diffusion of CCl_3F towards the aqueous droplets. The next condition is the undercooling of the emulsion in order to start the nucleation.

There are two reasons to concentrate the analysis on the aqueous droplets: first, the droplets are the locus where hydrate formation takes place, and second, the oil phase does not crystallize in the range of temperature imposed in the model.

2. Statement of the problem

In a previous work [1] the formation and dissociation of the CCl_3F hydrate was determined experimentally by differential scanning calorimetry (DSC). The formation and dissociation of the CCl_3F hydrate was detected upon heating of the emulsion, precisely, during the melting of the ice. The materials of the hydrate were the trichlorofluoromethane (CCl_3F) as the forming hydrate molecule and water. The system employed to carry out the CCl_3F hydrate formation was a w/o emulsion. First, the CCl_3F is dissolved in the oil phase, then in a second step the dispersion of the aqueous droplets is stabilized by means of a nonionic surfactant. The diffusion of the CCl_3F from the oil phase towards the aqueous droplets and the supercooling are necessary kinetic processes to begin the CCl_3F hydrate formation.

The study of CCl_3F hydrate is widely used in laboratory research because on the one hand, it forms the cage structure II [2] which is similar to the $CH_4 + C_2H_6$ hydrate. On the other hand, the formation of CCl_3F hydrate presents the induction time while ethane or acetylene hydrates do not have induction times [3]. Both aspects are crucial to gain insight in the knowledge of natural clathrate formation kinetics. Natural clathrate are mainly formed by methane gas, besides, their kinetic process of formation is strongly influenced by induction time.

The aim of this work is to determine the thermal history of a trichlorofluoromethane hydrate forming system during steady cooling. The model is based on the resolution of the continuity equation in terms of the heat balance which includes the source term and the probability of nucleation $J(T)$. The boundary volume of the w/o emulsion is a cylindrical crucible of a few mm^3 as shown in Fig. 1. The internal radius R of the crucible is small in comparison to its length L ($R \ll L$).

The aqueous droplets of the w/o emulsion are small enough to consider the liquid system inside the cylinder as homogeneous (mean droplet diameter = 60 μm). In order to simulate the steady cooling of the emulsion we imposed a constant cooling rate around the external surface of the boundary volume.

The industrial conditions applied to prevent the hydrate formation are turning from thermodynamic inhibitors such as methanol and electrolytes, to kinetic inhibitors such as surfactants and anti-agglomerants. The interest of this work

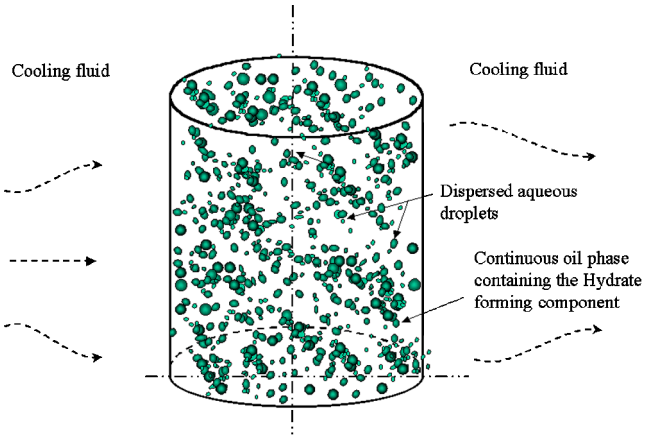

Fig. 1. Boundary volume of the system showing the distribution of the w/o emulsion within the domain.

to the real industrial needs lies in two facts: firstly, the present modeling deals with an emulsion, therefore, it is extendable to an actual need where a surfactant retards the kinetics of hydrate formation. Secondly, the approach of the modeling enables to link the thermodynamic aspects of hydrate formation with the kinetic aspects through the function $J(T)$.

Ehmimed et al. [4] measured the influence of the global heat transfer coefficient k on the rate of thermal transfer. In that work [4] the authors concluded that thermal transfer is influenced by the heat transfer coefficient only for values of k lower than 100 $\mathrm{W{\cdot}m^{-2}{\cdot}K^{-1}}$. The kind of crucible and the experimental conditions in this particular work are similar to that reported by Zeraouli [5]. The coefficient of heat transfer greater than 500 $\mathrm{W{\cdot}m^{-2}{\cdot}K^{-1}}$, so, it is possible to neglect the influence of the global heat transfer coefficient k on the rate of thermal transfer. In addition, the viscosity of the w/o emulsion allows to consider the liquid as a Newtonian fluid. Therefore, we can assume that the thermal transfer between the cooling fluid and the emulsion is not ruled by the global heat transfer coefficient k, neither by the viscosity of the emulsion.

In contrast, the thermal transfer is strongly influenced by an important amount of heat released during the formation of the solid hydrate. In consequence, the temperature distribution in the time interval of hydrate formation in the emulsion is determined by two effects:

(1) The external effect of the imposed steady cooling.
(2) The internal effect due to the exothermic heat released by the crystallization of the droplets.

For long, thin cylinders having negligible axial variations in heat flux, the gradient of heat transfer in the radial direction dominates over the axial. Since the geometry of the boundary volume fulfills this condition of $R \ll L$ we can focus the analysis on the heat transfer in radial direction. Additionally, since the emulsion is stable and the droplets are homogeneously distributed in the emulsion volume, we can assume that the temperatures of the w/o emulsion in radial direction are axisymmetrical [6,7]. The stability of the emulsion is broken when the hydrate is formed.

In this manner, the problem is to determine the temperature of the w/o emulsion $T(r,t)$ at any time t during the steady cooling, and for all position r between the center of the cylinder and the radius R.

The initial and final temperatures of the cooling interval are free parameter that must be specified. In this work, the steady cooling begins at 298 K and the lower limit of temperature is 240 K. The cooling rate denoted as β is 10 $\mathrm{K{\cdot}hr^{-1}}$. The dispersed phase of the emulsion crystallizes in this temperature interval, the oil phase of the emulsion remains at liquid state. The previous work [1] allows to establish this behavior of the w/o emulsion. Therefore, the numerical modeling of the thermal history is referred to the dispersed phase. Hereafter the continuity equation is expressed as an energy balance of the dispersed phase.

A heat source term is taken into consideration within the energy balance of the dispersed phase. During the thermal history of the dispersed phase, the onset time of crystallization initiates the release of heat inside the w/o emulsion. The source term depends on the probability of crystallization of every drop. The results of the steady cooling of an emulsion reveal that not all the droplets crystallize simultaneously. Actually, a progressive crystallization occurs and the rupture of the metastable state in the liquid phase is defined by the rate of nucleation $J(T)$ in every drop [8].

Hereafter Φ shall denote the mass fraction of the dispersed phase in the w/o emulsion. This parameter is the ratio of the mass of dispersed droplets to the total mass of emulsion. It is assumed that the thermal conductivity λ and the specific heat Cp do not vary in the range of temperatures of the cooling. Nevertheless, λ and Cp are considered dependent functions of the fraction of crystallized droplets φ in the emulsion. The fraction of dispersed droplets in solid state at position r and time t shall be denoted by $\varphi(r,t)$ and it varies between $0 \leqslant \varphi(r,t) \leqslant 1$. Therefore, from the work of Fouconnier et al. [10] a linear law of variation allows to write the following equations:

$$\lambda(\varphi) = \lambda_{\mathrm{l}} + (\lambda_{\mathrm{s}} - \lambda_{\mathrm{l}}) \tag{2.1}$$

$$Cp(\varphi) = Cp_{\mathrm{l}} + (Cp_{\mathrm{s}} - Cp_{\mathrm{l}}) \tag{2.2}$$

The thermal transfer during the cooling process of the w/o emulsion is modeled with the continuity equation of heat conduction:

$$\rho \cdot Cp \frac{\partial T}{\partial t} = \nabla(\lambda \nabla T) + \dot{q} \tag{2.3}$$

The heat source term $\dot{q}$ is different from zero at the onset time of droplet crystallization. The occurrence of such event at undercooling conditions is governed by a probabilistic law of nucleation [9,11,12]. Only when the probability of nucleation $J(T) > 0$ a fraction of the undercooled droplets crystallize $\varphi(r,t)$. The latent heat of solidification of the fraction $\varphi(r,t)$ represents the heat source term $\dot{q}$.

The solution of Eq. (2.3) enables the determination of the space–time distribution of temperature across the radial position in the cylinder $T(r,t)$. Before enterprising the solution of Eq. (2.3) it is important to point out the connection between the heat source term $\dot{q}$ and the probability of nucleation $J(T)$. In order to precise such a connection, it is convenient to remind the mechanisms of nucleation and crystallization that allow to derive an expression of the type $\dot{q} = J(T)$. Then, the continuity equation (2.3) can be expressed in terms of the dependent variable $T(r,t)$ and known functions.

3. Hydrate nucleation and crystallization

Most of the hydrate work focus on the equilibrium conditions of hydrate formation [13–18]. However, it has been confirmed since the nineteenth century that hydrate formation follows a complicated process of solidification. In this sense, there are still few works that deals with the kinetic aspects of hydrate formation. Two of the pioneering works that deals with the induction time concept are due to Englezos et al. [9] and the work of Natarajan et al. [19]. It is worthwhile to mention the experimental works of Jakobsen et al. [20], Lekvam and Ruoff [3], Munck et al. [21] and Zatsepina and Buffet [22]. The works aforementioned make evident the influence of the supercooling on hydrate formation kinetics. As those fine writers have shown, the gas hydrate is formed through a kinetic process which requires three necessary steps:

(1) The first one is supercooling. The aqueous solution saturated with the hydrate forming gas has to be cooled down to a temperature below the melting point of water. This lower level of temperature is named the nucleation temperature. The degree of undercooling is defined as the difference between the equilibrium temperature (or melting point T_F) and the nucleation temperature. At such conditions of undercooling, the molecular arrangement of water becomes more and more structured [23].
(2) The second step is nucleation. The water molecules begins to form orthogonal cage structures by means of hydrogen bonds. The orthogonal cages associates between them in order to form the nucleus surface which is the precursor of the solid phase. The clusters that are formed by the association of the orthogonal structures are relatively long-live entities ($1–10^3$ ps). In consequence, the clusters may dissociate and associate following a dynamic process in time [24–26]. During the nucleation stage although the crystal precursors are forming, no solid phase is still present in the undercooled liquid. The system is said to be in a metastable equilibrium.
(3) The third step is the growth of the crystal. Nucleation stage finishes at the moment when nuclei overcome an energy barrier necessary to reach a critical size [9,12]. Once a stable crystal embryo is formed, the next kinetic stage of hydrate formation is a process of crystal growth in three dimensions. If the viscosity of the supercooled liquid increases during the cooling effect, then the rate of crystal growth may be limited, on the contrary, if there is no influence of the viscosity on the crystal growth then the supercooling enhances the crystallization. At the moment of hydrate formation two phases coexist in the system, the solid phase (the hydrate) and the liquid phase (the hydrate forming molecules dissolved in the aqueous solution).

The supercooling phenomenon is characterized by the persistence in the liquid state of a material below its melting point T_F. However, the rupture of the metastable equilibrium of the supercooled liquid occurs at the beginning time of hydrate formation. One of the main parameters that has influence on the supercooling is the volume of the liquid. For example, a bulk volume of water of a few cm^3 is characterized by a supercooling degree of $\Delta T = -14$ K, while micro-droplets of water dispersed in a w/o emulsion (volumes of a fraction of μm^3) the crystallization occurs at 233 K or lower temperatures [5,6,25].

The steady cooling of a water-in-oil emulsion shows clearly the stochastic nature of crystallization. The experimental results of the steady cooling of an emulsion recorded by DSC reveals a gradual crystallization of the micro-droplets. The population of droplets solidifies gradually in a range of temperatures, i.e. not all the droplets crystallize simultaneously at the same temperature [5,7].

The cooling thermogram obtained by DSC is a plot of the heat changes within the emulsion in function of time. Fig. 2 shows a cooling thermogram of a w/o emulsion composed of water-in-vaseline [7]. When the crystallization takes place the heat signal describes an exothermic peak. The crystallization signal of the aqueous droplets of a w/o emulsion adopts the shape of a Gauss distribution. Therefore, the heat released in function of time shows that the crystallization of micro-droplets occurs gradually in a range of temperatures.

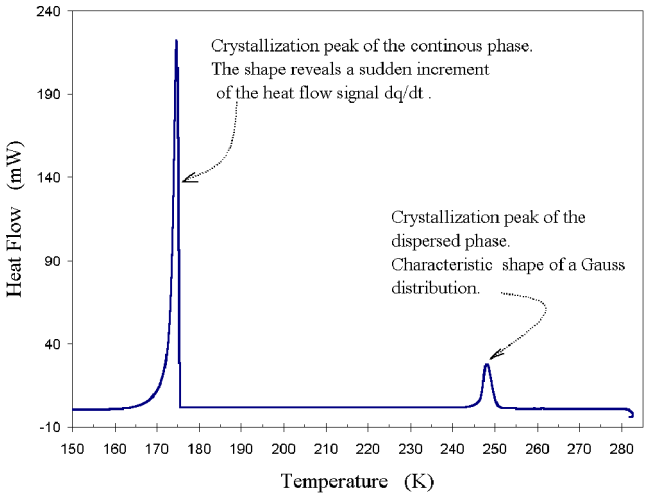

Fig. 2. Cooling thermogram of a w/o emulsion.

The summit of the Gaussian peak is considered as the most probable crystallization temperature T_c^* of the droplets. The progressive shape of the Gauss signal is due to the difference in size among all the droplets, hence, the release of heat during the crystallization is also pointed out by the gradual development in time of the peak.

From the moment of the beginning of solid formation (the appearance of the hydrate) the metastable equilibrium of the aqueous solution no longer exists. The occurrence of such instant in time is a phenomenon of random and probabilistic nature if the conditions of supercooling, pressure and composition are fulfilled [11,27]. At conditions of nucleation, it is not possible to determine the place where the nuclei are formed inside an aqueous droplet. Nevertheless, a probability $P = VJt$ of appearance of solid droplet can be predicted because it is possible to calculate the nucleation rate J [5,22].

The appearance of a nucleus is essentially a random phenomenon for which a probability can be predicted. If we consider a population of N aqueous droplets whose volumes are V, the nucleation will not occur in all the droplets at the same time as temperature decreases. Instead, the birth of nuclei occurs randomly. Let $n(r,t)$ be a fraction of N that represents the number of solidified droplets at position r and time t, then the proportion of solidified droplets in the total population of N at position r and time t is:

$$\varphi(r,t) = \frac{n(r,t)}{N} \tag{3.1}$$

and the number of droplets remaining in liquid state at time t is $N - n(r,t)$.

Assuming that each solidified droplet of n corresponds to the appearance of a nucleus, there is an equal probability of forming a nucleus in each of them. The probability of nucleation in a droplet of volume V in a time increment dt is $1VJ\,\mathrm{d}t$.

Let us consider not only one droplet but a large population composed of N droplets per unit volume of w/o emulsion. The water-in-oil emulsion is submitted to a steady cooling from a starting temperature of 298 K until an imposed temperature lower than T_F. At the beginning of the cooling all the droplets N are in liquid state, as the cooling progresses the metastable equilibrium will be broken at instant time t. In consequence, at time $t > 0$ there are $n(r,t)$ droplets in solid state per unit volume of w/o emulsion.

The rate of crystallization is proportional to the number of droplets remaining in liquid state, $N - n(r,t)$, and proportional also to the probability of crystallization by unit of time and volume $J(T)$. The rate of crystallization of those remaining droplets in a time increment dt is expressed as:

$$\frac{\mathrm{d}n(r,t)}{\mathrm{d}t} = \big[N - n(r,t)\big]J(T) \tag{3.2}$$

We can also express Eq. (3.2) in terms of the proportion of crystallized droplets $\varphi(r,t)$, then:

$$\frac{\mathrm{d}\varphi(r,t)}{\mathrm{d}t} = \big[1 - \varphi(r,t)\big]J(T) \tag{3.3}$$

Eq. (3.3) expresses the kinetics of crystallization of the dispersed droplets inside a w/o emulsion submitted to steady cooling.

4. Estimation of the rate of nucleation $J(T)$

In classical nucleation theories the rate of homogeneous nucleation J represents the number of nuclei formed per unit time and unit volume, the expression of $J(T)$ is given by:

$$J(T) = A\exp\left(-E + \frac{\Delta G}{kT}\right) \tag{4.1}$$

$J(T)$ is a nonlinear function of temperature T. For temperatures above the melting temperature the function $J(T)$ is close to zero. On the contrary, as supercooling increases $J(T)$ also increases exponentially and very quickly [8,28]. The coefficient E is a function of the viscosity of the liquid whereas ΔG is the energy barrier that nuclei must overcome in order to reach a stable critical size. The energy barrier is basically imposed by the interfacial tension between the nuclei and the liquid phase [12,29,30].

Moreover, if the viscosity of the liquid is too large in comparison to ΔG, then the value of E must be taken into consideration. A large value of E implies that the rate of nucleation is limited by viscosity. In this work, the viscosity of the w/o emulsion behaves as a Newtonian liquid, hence, it has a weak influence on the crystallization behavior of the dispersed phase [1]. It is assumed the following form of Eq. (4.1):

$$J(T) = A\exp\left(\frac{\Delta G}{kT}\right) \tag{4.2}$$

Quantifying the rate of hydrate nucleation is a difficult experimental problem. First, we must be able to detect the appearance of hydrate nuclei. Second, we need to observe a large number of nucleation events in order to obtain a meaningful statistical average for the nucleation rate.

The rate of nucleation can be determined by means of the differential scanning calorimetry technique (DSC) [6,31]. An experimental function as described by the following Eq. (4.3) can be fitted from measurements of temperature inside the crucible [5,8].

$$J(T) = A\exp\left(\frac{-B}{T(T - T_F)^2}\right) \tag{4.3}$$

To carry out the experimental procedure may turn most difficult than the determination of A and B. Several temperatures must be recorded at different positions inside the sample container, this implies the use of thermocouple in contact with the liquid. In this work such method was not followed since it requires very coercive experimental conditions inside the crucible. Nevertheless, it is also possible to determine the rate of nucleation employing the cooling-heating thermograms, the method gains in simplicity but looses in accuracy. The methodology has been employed previously

[5,27,32], and validated for cooling rates slow enough to assure that no gradient of temperature across the plate and the liquid sample exists.

A complete description of the method may be found in Refs. [5,27,32,33]. The main condition to validate the quantification of $J(T)$ by means of the cooling-heating thermogram is to use a cooling rate lower than 15 K·hr^{-1}. In this manner we can assume that the same temperature is maintained between the first layer of liquid inside the crucible and the surrounding resistance of the calorimeter [5].

Experimental data of a previous experimental work [1] allowed to determine the coefficients A and B of Eq. (4.3) from the hydrate formed upon heating during the melting of ice. The method described by Cordiez [27] is applied using the heating thermograms. Besides, the coefficients A and B determined from the results of that work [1] are applicable in the current model since formulation remains the same. The mean statistical values determined from the cooling-heating cycles carried out by DSC are $A = 3.12 \times 10^9$ nuclei·m^{-3}·s^{-1} and $B = 2.67 \times 10^6$ K^3.

5. Mathematical model and set of boundary conditions

5.1. Assumptions and derivation of the model

The nonlinear heat conduction of the dispersed phase of the w/o emulsion is defined by the model equation (2.3). Eq. (2.3) can be expressed in terms of the dependent variable $T(r,t)$, the rate of crystallization $J(T)$ and the fraction of crystallized droplets $\varphi(r,t)$. The precedent assumption of $R \ll L$ enables to consider a one-dimensional heat conduction in radial direction [34]. The analog form of Eq. (2.3) in cylindrical coordinates is:

$$\rho\, Cp \frac{\partial T(r,t)}{\partial t} = \frac{1}{r}\frac{\partial}{\partial r}\left(r\lambda(r,t)\frac{\partial T(r,t)}{\partial r}\right) + \dot{q}(r,t) \qquad (5.1)$$

The thermal properties of the dispersed phase defined in Eqs. (2.1) and (2.2) are linear functions of $\varphi(r,t)$. In this sense, during the steady cooling $\varphi(r,t) = 0$ for the time interval where the dispersed phase in the form of subcooled liquid. Nevertheless, from the moment of hydrate formation $\varphi(r,t) > 0$ and increases until $\varphi(r,t) = 1$. In consequence the thermal properties λ and Cp change in time.

In this sense, the rupture of the metastable equilibrium of the liquid droplets points out the beginning of hydrate formation. The source term is no longer $\dot{q} = 0$ in reason of the exothermic character of the phase transition. The heat flow per unit volume of dispersed phase (in J·m^{-3}·s^{-1}) is proportional to the kinetics of crystallization. The relation between $\dot{q}(r,t)$ and the kinetics of crystallization can be expressed as follows:

$$\dot{q} = \rho L \frac{\mathrm{d}\varphi(r,t)}{\mathrm{d}t} \qquad (5.2)$$

where L is the apparent latent heat of the dispersed phase.

5.2. The boundary conditions

The temperature of the cooling fluid decreases at a constant rate, at $t = 0$, $T_\infty(0) > 0$ where T_F is the melting temperature of the dispersed phase. At any time $t > 0$ the external surface is always in contact with the cooling fluid at $T_\infty(t)$, therefore:

$$T(r,t) = T_\infty(t) \quad \text{at } r = R \text{ and } t > 0$$

The condition of axisymmetrical temperatures in relation to r imposes:

$$\frac{\partial T(r,t)}{\partial r} = 0 \quad \text{at } r = 0 \text{ and } t > 0$$

5.3. The initial conditions

$$T(r,t) = T_\infty(0) > T_F \quad \text{for } 0 < r < R,\ t = 0$$
$$\varphi(r,t) = 0 \quad \text{for } 0 < r < R,\ t = 0$$

6. Numerical solution of the model equation

Eq. (5.1) of heat conduction can be solved by means of a numerical algorithm for $T(r,t)$. Here we choose an explicit forward finite difference method for the solution of the partial differential equation (5.1). In order to determine $T(r,t)$ in the radial direction during the cooling, the position coordinate r and the time t are represented by discrete set points m and i respectively,

$$i = 1, 2, 3, \ldots, I \quad \text{for}$$
$$t_1 = 0,\ t_2 = t_1 + \Delta t,\ t_3 = t_1 + 2\Delta t, \ldots, t_{\text{end}}$$
$$m = 1, 2, 3, \ldots, M \quad \text{for}$$
$$r_1 = 0,\ r_2 = r_1 + \Delta r,\ r_3 = r_1 + 2\Delta r, \ldots, R$$

Thus, the coordinate r in radial direction is represented by a dimensional grid shown in Fig. 3. The center of the radius $r = 0$ is assigned with the node $m = 1$, each node spans the radius with a fixed radial length Δr. At radius R the corresponding node is M. The duration of time of the cooling experiment is also discretized by constant time steps Δt. The cooling experiments begin at $t = 0$ that corresponds in the time grid to $i = 1$, the final instant of the experiment t_{end} in the finite difference representation corresponds to $i = I$. Hereafter we denote the temperature and the crystallized fraction in node m and time i as Θ_m^i and φ_m^i respectively. The explicit forward scheme means that Θ_m^{i+1} for each m can be calculated explicitly from the quantities that are already known. The requirement of stability to maintain convergence is:

$$\frac{\Delta t}{\Delta(r)^2} \leqslant \frac{\rho \min(Cp_l, Cp_s)}{4\max(\lambda_l, \lambda_s)} \qquad (6.1)$$

The solution of the nonlinear second order partial differential equation (5.1) is carried out by means of the explicit finite difference approach. The resultant equations are as follows:

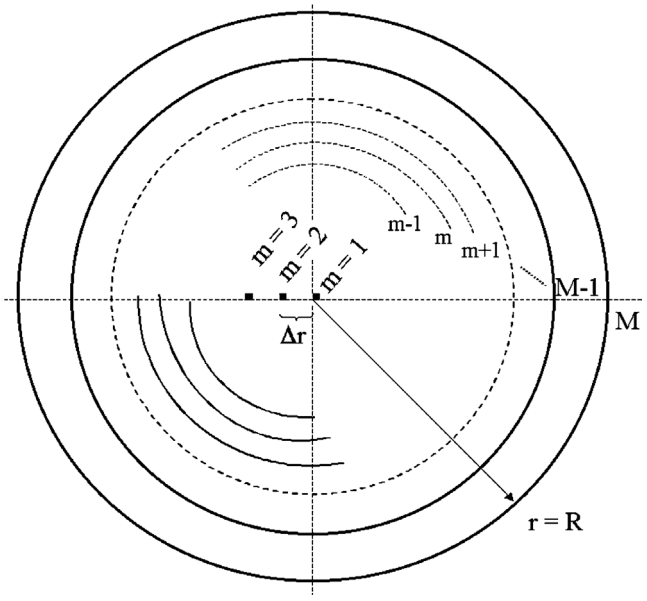

Fig. 3. Grid of the boundary volume in radial direction.

$$\Delta r = \frac{2R}{2M-1} \tag{6.2}$$

$$\Delta t = \frac{T}{I-1} \tag{6.3}$$

$$\Theta_m^{i+1} = \Theta_1^i + L\Delta t \frac{1}{Cp_1^i}\left(1-\varphi_1^i\right) J\left(\Theta_1^i\right) + 4\frac{\Delta t}{\rho(\Delta r)^2}\frac{\lambda_1^i}{Cp_1^i}\left(\Theta_2^i - \Theta_1^i\right) \tag{6.4}$$

$$\Theta_m^{i+1} = \Theta_m^i + L\Delta t \frac{1}{Cp_1^i}\left(1-\varphi_1^i\right) J\left(\Theta_1^i\right) + \frac{\Delta t}{\rho(\Delta r)^2}\frac{\lambda_m^i}{Cp_m^i}\left(\Theta_{m+1}^i - 2\Theta_m^i + \Theta_{m-1}^i\right) + \frac{\Delta t}{\rho(\Delta r)^2}\frac{1}{2m-2}\frac{\lambda_m^i}{Cp_m^i}\left(\Theta_{m+1}^i - \Theta_{m-1}^i\right) \tag{6.5}$$

$$\Theta_{M+1}^i = \Theta_\infty^{i+1} \tag{6.6}$$

$$\Theta_m^i = \Theta_m^i + \left(1-\Theta_m^i\right) J\left(\Theta_{M+1}^i\right)\Delta t \tag{6.7}$$

The boundary conditions in discretized terms are:

$$\Theta_{M+1}^{i+1} = \Theta_\infty^{i+1} \quad \text{for } m = 1, 2, 3, \ldots, M$$

$$\Theta_M^i = \Theta_\infty^i \quad \text{for } i = 1, 2, 3, \ldots, I$$

$$\Theta_m^1 = 0 \quad \text{for } m = 1, 2, 3, \ldots, M$$

The numerical calculations were performed using a Fortran programming. The step size in time is $\Delta t = 1.25 \times 10^{-4}$ s and 40 radial positions are considered for Δr.

7. Results of the numerical simulation

The evolution of the temperature $T(r,t)$ of the dispersed phase is obtained from the numerical solution of Eqs. (6.4) and (6.5). The parameters used in the modeling are listed in Table 1. The thermo-physical properties of the dispersed phase are listed in Table 2, they were measured experimentally during a previous experimental work [1]. The water-in-oil emulsion contains $\Phi = 62.4\%$ mass of aqueous droplets stabilized by a nonionic surfactant. The dispersing solvent is a mixture of linear alkanes with a melting temperature $T_m < 183$ K.

Table 1
Parameters used in the modeling of the cooling of the w/o emulsion

Symbol	Value	Units
β	10	$K{\cdot}hr^{-1}$
$T_\infty(0)$	298	K
T_{end}	236	K
Δt	0.000125	s
Δr	0.0005125	m
M	40	Number of radial positions
R	20.5	mm

Table 2
Thermochemical properties of the dispersed phase of the w/o emulsion

Symbol	Value	Units
Φ	62.4	wt%
ρ	194.6748	$kg{\cdot}m^{-3}$
A	3.12×10^9	$Nuclei{\cdot}m^{-3}{\cdot}s^{-1}$
B	2.67×10^6	K^3
λ_s	2.6973	$W{\cdot}m^{-1}{\cdot}K^{-1}$
λ_l	0.46022	$W{\cdot}m^{-1}{\cdot}K^{-1}$
Cp_s	1.6628	$kJ{\cdot}kg^{-1}{\cdot}K^{-1}$
Cp_l	4.029855	$kJ{\cdot}kg^{-1}{\cdot}K^{-1}$
L	129.32	$kJ{\cdot}kg^{-1}$
T_F	253	K

Before starting the cooling experiments, the temperature of the sample is homogeneous inside the boundary volume and equal to $T_\infty(0) = 298$ K. Then, from $t = 0$ a constant steady cooling process is imposed on the external surface of the boundary volume. The temperature of the cooling fluid decreases linearly at a constant cooling rate of $\beta = 10$ $K{\cdot}hr^{-1}$. The lower limit of temperature reached in the cooling simulation is $T_{end} = T(r,t) = 236$ K.

The result of a simulation of the cooling process for radial positions $r = 0$ and $r = R$ is shown in Fig. 4. The evolution of the curve $T(r,t)$ reveals three different behaviors. The first one in the time interval $0 < t < 5$ hr presents the profile of a continuous cooling. During this first stage the fraction of solidified droplets is zero, $\varphi(r,t) = 0$. The second time interval between 5 hr $< t <$ 20 hr presents a different slope of the curve $T(r,t)$. The sudden change of slope at $t = 5$ hr indicates the onset time of hydrate crystallization.

From the beginning of the second stage $t = 5$ hr the fraction of solidified droplets starts to increase $\varphi(r,t) > 0$. This implies that formation of solid hydrate is occurring in the dispersed phase of the w/o emulsion. The fraction $\varphi(r,t)$ shall vary until it reaches the magnitude $\varphi = 1$. Correspondingly, an amount of heat is released

as hydrate crystallization progresses in the large population of droplets. The heat balance between the imposed steady cooling and the exothermic heat of crystallization results in the change of slope of $T(r,t)$ which is almost horizontal.

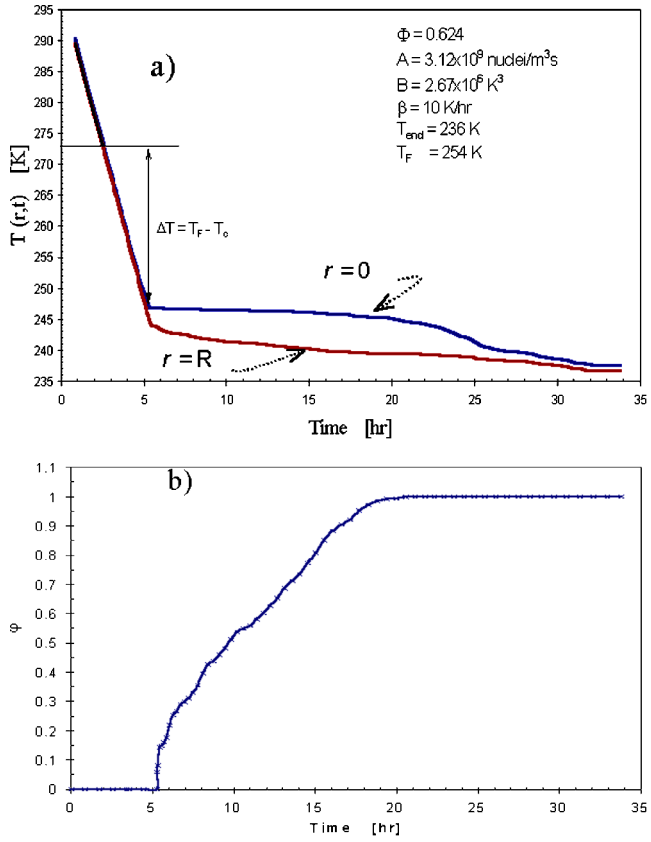

Fig. 4. (a) Evolution of temperature during the cooling of the w/o emulsion at positions $r = 0$ and $r = R$. (b) Evolution of the fraction of solidified droplets φ.

The third stage is also characterized by a change in the slope. From Fig. 4 it can be seen that for the innermost position $r = 0$ the stabilizing effect disappears at $t > 20$ hr. From this moment the cooling tendency becomes once again more important than the heat released. The behavior of $T(r,t)$ for the external position $r = R$ is nearly constant due to the proximity with the cooling fluid. Nevertheless, a last change in the slope is observed at $t > 25$ hr.

Moreover, Fig. 4 shows that the w/o emulsion at position $r = R$ reaches the lower temperatures in a shorter time than the emulsion at the center of the cylinder. The onset time of crystallization for both positions occurs almost simultaneously at $t = 5$ hr, however, the dispersed phase at the center of the cylinder crystallizes at $T = 246$ K meanwhile for $r = R$ it crystallizes at $T = 244$ K.

The evolution of temperature of the dispersed phase for the 40 radial positions inside the cylinder are shown in Fig. 5. The surface $T(r,t)$ exhibits the evolution of temperature from the less cold location $r = 0$ up to the most cold position $r = R$. We can also identify the onset time of hydrate crystallization at $t = 5$ hr.

The constant coefficients A and B in the function $J(T)$ define the influence of the volume of crystal and the interfacial tension liquid–crystal on the process of hydrate crystallization respectively. The model equation is solved for $A \pm 40\%$ and $B \pm 15\%$, the results are shown in Figs. 6 and 7 respectively. From Fig. 6 it can be pointed out that a variation of $+40\%$ in A leads to a faster decrease of temperature and hence, to a shorter time of crystallization. Similarly, when the coefficient B-15% is employed, the onset time of crystallization arrives at $T = 248$ K which is 4 degrees before the observed temperature for B, i.e. the magnitude of the supercooling is reduced. Therefore, the behavior of $T(r,t)$ is more sensible to the changes in B than A, in particular the supercooling degree allows to establish this conclusion.

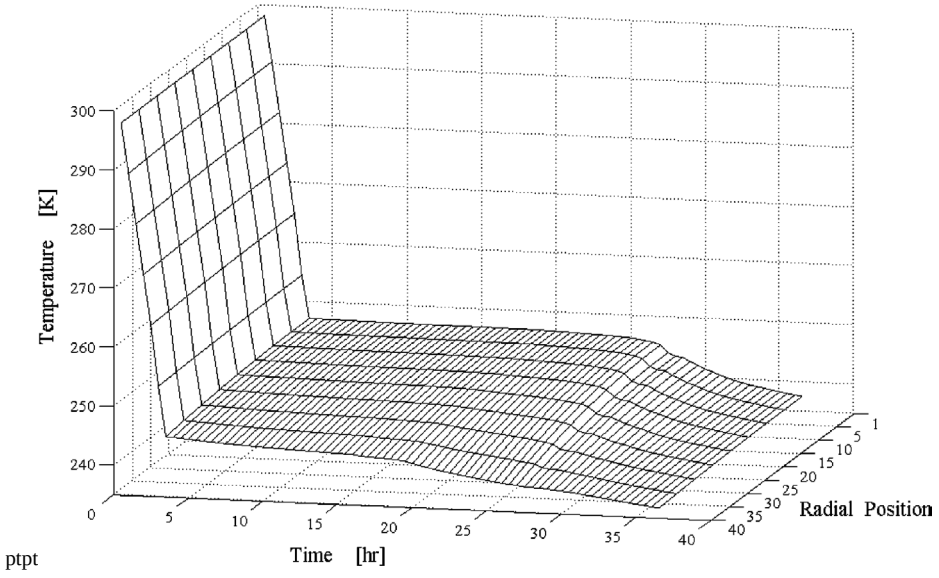

Fig. 5. Temperature evolution in time and radial position of the dispersed phase. The first change of slope indicates the beginning of the hydrate crystallization.

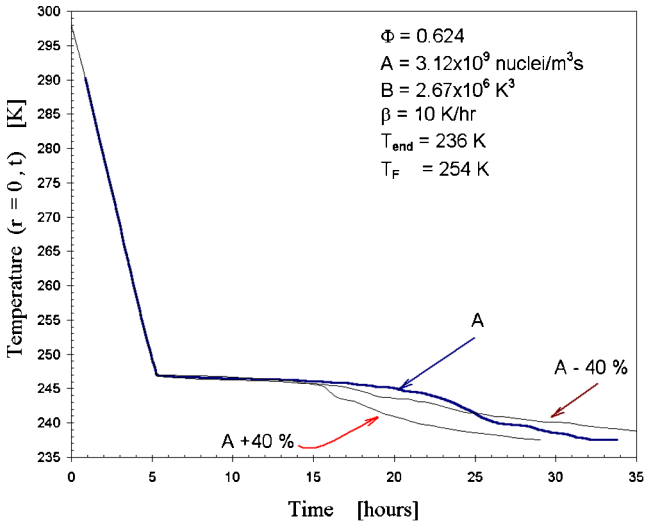

Fig. 6. Influence of coefficient A on the temperature history.

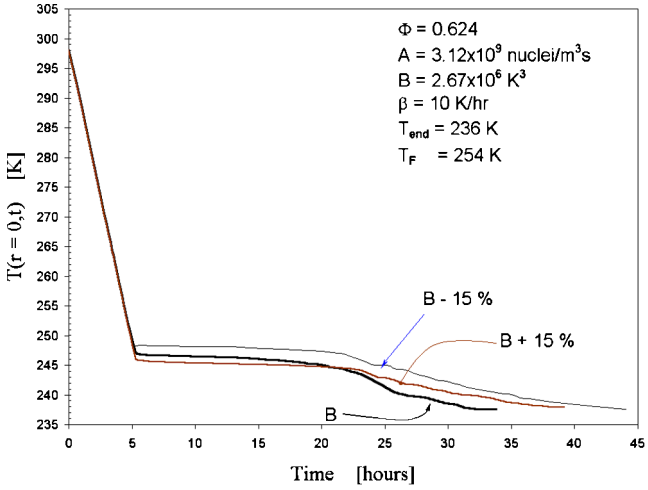

Fig. 7. Influence of coefficient B on the evolution of the temperature.

8. Conclusions

The evolution of temperature inside an hydrate forming system is modeled in this work. The study system is a w/o emulsion, the CCl_3F is the hydrate forming molecule and the CCl_3F hydrate formation takes place in the dispersed droplets of the emulsion. The model equation is based on the resolution of the continuity equation in terms of a heat balance. Each term of the model equation is stated for the heat balance in the dispersed phase. The boundary condition imposed to the study system is a steady cooling from 298 K down to 236 K at a constant cooling rate of 10 $K{\cdot}hr^{-1}$. The model equation considers the heat source term in virtue of the heat released by the crystallization. The rate of heat released is in turn a function which depends on the probability of nucleation $J(T)$. The crystallization implies to specify a term which takes into account the random and probabilistic nature of nucleation. Such a term is the function $J(T)$ that was derived from experimental DSC measurements carried out in a previous work [1] in a w/o emulsion. The model equation is solved by a numerical explicit scheme. The results provided by the modeling allows to depict three stages during the cooling process: The first stage is characterized by the steady cooling tendency. The second stage is mainly characterized by the starting point of hydrate nucleation. In this second stage an stabilizing effect is observed as a result of a balance between the steady cooling and the energy released by crystallization. The third stage occurs at lower temperatures, the heat released by the crystallization become less influent and the cooling tendency prevails. The results make evident the strong influence of the supercooling on the onset time of hydrate crystallization. This work enhances the scope to resolve the question whether hydrate can form at a given conditions of supercooling. The equilibrium conditions stated by thermodynamics can be linked with an approach that considers the probabilistic nature of crystallization in order to better predict the hydrate formation. The link we refer to becomes possible through the term $\Delta G/(kT)$ expressed in the rate of nucleation $J(T)$.

References

[1] D. Clausse, B. Fouconnier, J. Avendaño-Gomez, Ripening phenomena in emulsions—a calorimetry investigation, J. Dispersion Sci. Technol. 23 (2003) 379–391.
[2] E.D. Sloan, F. Fleyfel, Hydrate dissociation enthalpy and guest size, Fluid Phase Equilibria 76 (1992) 123–140.
[3] K. Lekvam, P. Ruoff, A reaction kinetic mechanism for methane hydrate formation in liquid water, J. Amer. Chem. Soc. 115 (1993) 8565–8569.
[4] J.A. Ehmimed, Y. Zeraouli, J.P. Dumas, A. Mimet, Heat transfers model during the crystallization of a dispersed binary solution, Int. J. Thermal Sci. 42 (2003) 33–46.
[5] Y. Zeraouli, Étude thermique des transformations des emulsions concentrées: application à la calorimetrie à balayage, PhD thesis, Université de Pau et Pays de l'Adour, France, 1981.
[6] D. Clausse, Research Techniques Utilizing Emulsions, Encyclopedia of Emulsion Technology, vol. 2, Marcel Dekker, New York, 1985.
[7] D. Clausse, Thermal behavior of emulsions studied by differential scanning calorimetry, J. Thermal Anal. 51 (1998) 191–201.
[8] S. Gibout, M. Strub, J.P. Dumas, Estimation of the nucleation probability in emulsions, Int. J. Heat Mass Transfer 47 (2004) 63–74.
[9] P. Englezos, N. Kalogerakis, P.D. Dholobhai, P.R. Bishnoi, Kinetics of formation of methane and ethane gas hydrates, Chem. Engrg. Sci. 42 (11) (1987) 2647–2658.
[10] B. Fouconnier, Y. Manissol, D. Dalmazzone, D. Clausse, Study of trichlorofluoromethane hydrate formation in w/o emulsions: dissociation energy and equilibria with salt + water solutions, Entropie 239/240 (2002) 72–77.
[11] G.F. Frank, J.Z. Chao, B.R. Andrew, D.C. Xiao, J.C. John, R. Lindsay, Simulation and experiment of the unsteady heat transport in the onset time of nucleation and crystallization of ice from the subcooled solution, Int. J. Heat Mass Transfer 46 (2003) 3221–3231.
[12] D. Frenkel, Old and new phases in complex liquids, Revue de l'Institut Francais du Petrole 51 (1) (1996).
[13] A. Chapoy, C. Coquelet, D. Richon, Solubility measurement and modeling of water in the gas phase of the methane/water binary system at temperatures from 283.08 to 318.12 K and pressures up to 34.5 Mpa, Fluid Phase Equilibria 214 (2003) 101–117.
[14] P. Englezos, N. Kalogerakis, P.R. Bishnoi, Simultaneous regression of binary VLE and VLLE data, Fluid Phase Equilibria 61 (1990) 1–15.

[15] P. Englezos, N. Kalogerakis, M.A. Trebble, P.R. Bishnoi, Estimation of multiple binary interaction parameters in equations of state using VLE data. Application to the Trebble–Bishnoi equation of state, Fluid Phase Equilibria 58 (1990) 117–132.
[16] P. Englezos, P.R. Bishnoi, Gibbs free energy analysis for the supersaturation limits of methane in liquid water and the hydrate–gas–liquid water phase behavior, Fluid Phase Equilibria 42 (1988) 129–140.
[17] G.D. Holder, P.M. Lakshmi, R.P. Warzinski, Formation of gas hydrates from single phase aqueous solutions, Chem. Engrg. Sci. 56 (2001) 6897–6903.
[18] J.B. Klauda, S.I. Sandler, A fugacity model for gas hydrate phase equilibria, Ind. Engrg. Chem. Res. 39 (2000) 3377–3386.
[19] V. Natarajan, P.R. Bishnoi, N. Kalogerakis, Induction phenomena in gas hydrate nucleation, Chem. Engrg. Sci. 49 (13) (1994) 2075–2087.
[20] T. Jakobsen, J. Sjöblom, P. Ruoff, Kinetics of gas hydrate formation in w/o emulsions. The model system trichlorofluoromethane/water/non-ionic surfactant by means of dielectric spectroscopy, Colloids and Surfaces, A: Physicochemical and Engineering Aspects 112 (1996) 73–84.
[21] J. Munck, S. Skjold-Jorgensen, P. Rasmunsen, Computations of the formation of gas hydrates, Chem. Engrg. Sci. 43 (10) (1988) 2661–2672.
[22] O.Y. Zatsepina, B.A. Buffet, Nucleation of CO_2 hydrate in porous medium, Fluid Phase Equilibria 200 (2002) 263–275.
[23] C.A. Koh, R.P. Wisbey, W. Xiaouping, R.E. Westacott, Water ordering around methane during hydrate formation, J. Chem. Phys. 113 (2000) 6390–6397.
[24] B. Fouconnier, V. Legrand, L. Komunger, D. Clausse, L. Bergfoldt, J. Sjöblom, Formation of trichlorofluoromethane hydrate in w/o emulsions studied by differential scanning calorimetry, Progr. Colloid Polym. Sci. 112 (1999) 105–108.
[25] B. Fouconnier, J. Avendano-Gomez, K. Ballerat-Busserolles, D. Clausse, Thermal Behaviour of Dispersed Systems, Marcel Dekker, New York, 2000.
[26] E.D. Sloan, Clathrate hydrate measurements: microscopic, mesoscopic, and macroscopic, J. Chem. Thermodyn. 35 (2003) 41–53.
[27] J.P. Cordiez, Contribution à l'étude des phenomenes de nucleation en bain surfondu. Étude de l'acide stearique en emulsion dans l'eau, PhD thesis, Universite Aix Marseille, France, 1981.
[28] R.A. Lambert, R.H. Rangel, Solidification of a supercooled liquid in stagnation-point flow, Int. J. Heat Mass Transfer 46 (2003) 4013–4021.
[29] M. Sugaya, Y.H. Mori, Behavior of clathrate hydrate formation at the boundary of liquid water and a fluorocarbon in liquid or vapor state, Chem. Engrg. Sci. 51 (1996) 3505–3517.
[30] H.T. Nguyen, N. Kommareddi, V.T. John, A thermodynamic model to predict clathrate hydrate formation in water-in-oil microemulsion systems, J. Colloid Int. Sci. 155 (1993) 482–487.
[31] H. Suga, Calorimetric studies of some energy related materials, Termochim. Acta 328 (1999) 9–17.
[32] C. Dalmazzone, Differential scanning calorimetry: a new technique to characterize hydrate formation in drilling muds, SPE 62962 (2000).
[33] F. Danes, B. Garnier, Estimating heat transfer bias of kinetic measurement for polymers by differential scanning calorimetry with isothermal mode, Int. J. Thermal Sci. 42 (2003) 583–590.
[34] M.H. Hussain, I. Dincer, Two-dimensional heat and moisture transfer analysis of a cylindrical moist object subject to drying: a finite-difference approach, Int. J. Heat Mass Transfer 46 (2003) 4033–4039.